

# Plug and Thermal Barrier Potential Formations in a Tandem Mirror

KATANUMA Isao, TATEMATSU Yoshinori, ISHII Kameo, SAITO Teruo and YATSU Kiyoshi

Plasma Research Center, University of Tsukuba, Tsukuba, Ibaraki 305-8577, Japan

(Received 15 October 2001 / Accepted 24 October 2001)

It is shown that plug and thermal barrier potentials are created simultaneously by electron cyclotron resonance heating (ECRH) in the end-mirror cells of a tandem mirror without a high energy sloshing ion population. Monte-Carlo particle simulation is carried out to investigate the electrostatic potential formation in the steady state in the end-mirror cell. It is found that a combination of the plug and thermal barrier potentials can be created using a two-component distribution of electrons at the inner mirror throat and a non-Maxwellian distribution of electrons which are heated by the plug ECRH and trapped magnetically in the thermal barrier region. In addition to the electron distributions, the potential formations require the existence of non-Maxwellian ions trapped in the thermal barrier potential which are assumed to be lost radially.

**Keywords:** plug, thermal barrier, potential, electrostatic potential, tandem mirror.

We have shown that a plug potential can be formed with the effects of non-Maxwellian electrons and ions which are trapped magnetically and electrostatically in the end-mirror cell in addition to Maxwellian ions and electrons flowing from the central cell of a tandem mirror [1]. In this calculation, only the region from the thermal barrier to the outer mirror throat in the end-mirror cell was considered with the thermal barrier potential depth as a given parameter.

In the tandem mirror experiments, however, plug potential formation is accompanied by the formation of the thermal barrier potential depth. Therefore, simultaneous calculation is necessary in the region from the inner mirror throat  $z = z_i$  to the outer mirror throat  $z = z_m$ , as shown in Fig. 1, for complete understanding of the electrostatic potential formation in the end-mirror cell.

The electron distribution function in the end-mirror cell is assumed as,

$$f_e = \begin{cases} n_{ew} \exp\left\{-\frac{\varepsilon + e\phi_i}{T_{ew}}\right\} + n_{ec} \exp\left\{-\frac{\varepsilon + e\phi_i}{T_{ec}}\right\} & \text{for } \varepsilon \geq \mu B_i - e\phi_i \\ n_{ew} \exp\left\{-\frac{\varepsilon + e\phi_i - \alpha_e \mu B_i}{(1 - \alpha_e)T_{ew}}\right\} & \text{for } \varepsilon < \mu B_i - e\phi_i \end{cases} \quad (1)$$

Here,  $\alpha_e$  is a constant, and the schematic diagram shown in Fig. 1(b) is considered. The standard no-

author's e-mail: katanuma@prc.tsukuba.ac.jp

tations are used such that  $B$  is magnetic field,  $\phi$  electrostatic potential,  $\varepsilon$  electron energy, and  $\mu$  magnetic moment. The normalization factor  $(m_e/2\pi T_e)^{3/2}$  of the distribution function is omitted through out this paper for the sake of simplicity. The electrons denoted by the density  $n_{ec}$  in Eq. (1) are a component of cold electrons at the inner mirror throat, which do not reach the thermal barrier  $z = z_b$  due to low kinetic energy, while the electrons denoted by the density  $n_{ew}$  is a component of warm electrons, which are heated by ECRH and escape from the plug region  $z \approx z_p$  to the inner mirror throat. The distribution function of the magnetically trapped electrons is connected continuously with that of warm electrons across  $\varepsilon = \mu B_i - e\phi_i$  in Figs. 1(b) and 1(c).

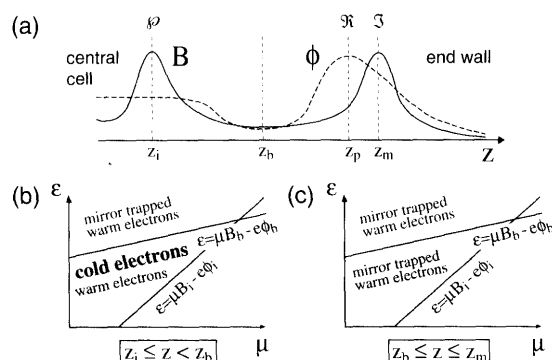


Fig. 1 Schematic diagram of plug/barrier region (a), and electron velocity space in the regions  $z_i \leq z < z_b$  (b) and  $z_b \leq z \leq z_m$  (c).

These two components of the electron distribution function have been observed in the experiments of the plug potential formation in the GAMMA10 tandem mirror [2].

Using Eq. (1) we obtain a modified Boltzmann law as

$$\frac{e(\phi - \phi_b)}{T_{ec}} = (1 - \alpha_e) \ln \left\{ \frac{B_b(B - \alpha_e B_i) n_e(z)}{B(B_b - \alpha_e B_i) n_{eb}} \right\}, \quad (2)$$

$$\frac{e(\phi - \phi_i)}{T_{ew}} = \left\{ \frac{\left(\frac{n_{ec}}{n_{ew}}\right) + 1 + \frac{\alpha_e(B_i - B)}{(B - \alpha_e B_i)} \left(\frac{B_i - B}{B_i}\right)^{1/2}}{\left(\frac{n_{ec} T_{ew}}{n_{ew} T_{ec}}\right) + 1 + \frac{\alpha_e B_i}{(B - \alpha_e B_i)} \left(\frac{B_i - B}{B_i}\right)^{1/2}} \right\} \times \ln \left\{ \frac{1}{\frac{n_{ec}}{n_{ew}} + \left[ 1 + \frac{\alpha_e(B_i - B)}{(B - \alpha_e B_i)} \left(\frac{B_i - B}{B_i}\right)^{1/2} \right]} \frac{n_e(z)}{n_{ew}} \right\}, \quad (3)$$

where Eq. (2) is applied in the region  $z_b \leq z \leq z_m$ , while Eq. (3) is in the region  $z_i \leq z < z_b$ . Here  $n_{eb}$  in Eq. (2) is the electron density at  $z = z_b$ . Equation (2) can also be derived with the assumption of a bi-Maxwellian electron distribution function, i.e.,  $f_e = n_{eb} \exp\{-\frac{1}{2}m_e v_{\parallel}^2/T_{c\parallel} - \frac{1}{2}m_e v_{\perp}^2/T_{e\perp}\}$ , where  $T_{c\parallel} = (1 - \alpha_e)T_{ew}$  and  $T_{e\perp} = (1 - \alpha_e)T_{ew} / (1 - \alpha_e B_i/B_b)$ . That is, the constant  $\alpha_e$  in Eq. (1) is related to the temperatures of magnetically trapped warm electrons in the thermal barrier region as  $\alpha_e = \frac{B_b}{B_i} \left(1 - \frac{T_{c\parallel}}{T_{e\perp}}\right)$ .

The electrostatic potential distribution is determined using Eqs. (2) and (3) if the electron density  $n_e(z)$  can be numerically calculated. For this, we use the charge neutrality condition  $n_e(z) = n_i(z)$ . The ion density is calculated using a Monte-Carlo code [3]. Coulomb collisions are included. The effects of radial loss of ions trapped in the thermal barrier region are included by setting a mean life time of  $\tau_{loss}$ . The ions are supplied at  $z = z_i$  continuously accompanied by a half-Maxwellian, i.e.,  $v_{\parallel} \geq 0$ , of temperature  $T_i$ .

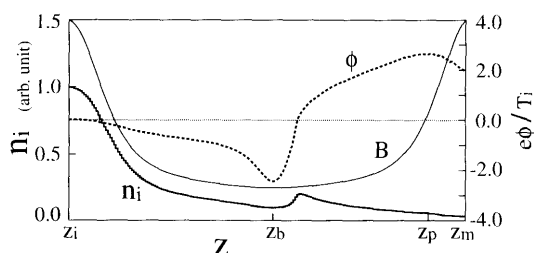


Fig. 2 Electrostatic potential and ion density axial profiles in the end-mirror cell, which were obtained by the Monte-Carlo simulation.

Figure 2 shows the calculation results. Here the parameters are  $n_{ec}/(n_{ec} + n_{ew}) = 0.96$ ,  $T_{ec}/T_{ew} = 0.2$ ,

$T_i/T_{ew} = 0.5$ , and  $T_{e\perp}/T_{c\parallel} = 50$ . Those parameters are not contradictory to the observations in the GAMMA10 experiments [2]. The ion loss time is  $\tau_{loss}/\tau_D = 0.18$ , where  $\tau_D$  is the coulomb deflection times defined as  $\tau_D \equiv \sqrt{m_i} T_i^{3/2} / (\sqrt{2} \pi n_0 e^4 \ln \Lambda_{ij})$ . Transit time  $\tau_{transit}$  necessary for thermal ions to move from  $z = z_i$  to  $z = z_m$  is  $\tau_{transit}/\tau_D \simeq 4.4 \times 10^{-3}$ , so that the relation  $\tau_{transit} \ll \tau_{loss} \lesssim \tau_D$  is satisfied.

It is seen that the plug and thermal barrier potentials are created in Fig. 2. The thermal barrier depth is deeper than the prediction from the Boltzmann law of cold electrons, i.e.,  $e(\phi_i - \phi_b) > T_{ec} \ln\{n_{ec}/n_{eb}\}$ , and the height of the plug potential is larger than the thermal barrier depth, i.e.,  $e(\phi_p - \phi_i) \geq e(\phi_i - \phi_b)$ , which are consistent with the observations from the GAMMA10 experiments.

The plug potential has sufficient height to confine the ions from the central cell because  $e(\phi_p - \phi_i)/T_i \simeq 2.6$ . The ion density gradually decreases from  $z = z_i$  toward  $z = z_m$ , which clearly satisfies the relation  $n_i(z_i) \gg n_i(z_b) \geq n_i(z_p)$ .

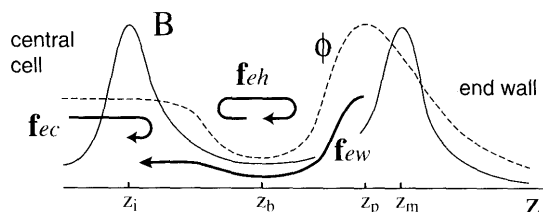


Fig. 3 Schematic diagram of electron orbits.

Figure 3 shows the schematic diagram of electron orbits which are responsible for the formations of the plug and thermal barrier potentials. Here  $f_{ec}$  is the orbit of the cold component of electrons in the central cell,  $f_{ew}$  is the orbit of the warm component of electrons at the inner mirror throat which are heated by ECRH around plug and escape from the plug/thermal barrier region,  $f_{eh}$  is the magnetically trapped non-Maxwellian electrons the distribution function of which is connected continuously with that of warm electrons.

If the cold electron component does not exist, only the deep thermal barrier potential is created. That is, the profile of electrostatic potential is almost symmetric about  $z = z_b$  so that the plug potential is not formed without cold electrons. The coulomb pitch angle collisions are important for the plug potential formation to attain  $|dn_i(z)/dz| \neq \infty$  at  $z = z_p$  in the calculation of this paper, as indicated in Ref. 1.

Radial loss of ions, which is included in this calculation as  $\tau_{\text{loss}}$ , is necessary for steady state potential formation. In GAMMA10, the plug/barrier potential structure can be sustained for 150 ms and no barrier filling has been observed [4]. This strongly suggests the radial loss of ions in GAMMA10 experiments.

In summary, it has been shown that the existence of the three components of electrons of  $f_{ec}$ ,  $f_{ew}$ , and  $f_{eh}$  as shown in Fig. 3 in addition to the coulomb collisions of ions around  $z = z_p$  and the ion radial loss in the end-mirror cell leads to the formation of plug and thermal barrier potentials.

- [1] I. Katanuma *et al.*, *will appear in J. Plas. Fus. Res.*  
I. Katanuma *et al.*, *submitted to Phys. Plasmas.*
- [2] T. Cho *et al.*, *Nucl. Fusion* **41**, 1161 (2001).
- [3] R. Minai *et al.*, *J. Phys. Soc. Jpn.* **66**, 2051 (1997).
- [4] K. Yatsu *et al.*, *Nucl. Fusion* **41**, 613 (2001).